

Machine Learning based Efficient QT-MTT Partitioning Scheme for VVC Intra Encoders

Alexandre Tissier, Wassim Hamidouche, Souhail Belhadj Dit Mdalsi, Jarno Vanne, Franck Galpin and Daniel Menard

Abstract—The next-generation Versatile Video Coding (VVC) standard introduces a new Multi-Type Tree (MTT) block partitioning structure that supports Binary-Tree (BT) and Ternary-Tree (TT) splits in both vertical and horizontal directions. This new approach leads to five possible splits at each block depth and thereby improves the coding efficiency of VVC over that of the preceding High Efficiency Video Coding (HEVC) standard, which only supports Quad-Tree (QT) partitioning with a single split per block depth. However, MTT also has brought a considerable impact on encoder computational complexity. In this paper, a two-stage learning-based technique is proposed to tackle the complexity overhead of MTT in VVC intra encoders. In our scheme, the input block is first processed by a Convolutional Neural Network (CNN) to predict its spatial features through a vector of probabilities describing the partition at each 4×4 edge. Subsequently, a Decision Tree (DT) model leverages this vector of spatial features to predict the most likely splits at each block. Finally, based on this prediction, only the N most likely splits are processed by the Rate-Distortion (RD) process of the encoder. In order to train our CNN and DT models on a wide range of image contents, we also propose a public VVC frame partitioning dataset based on existing image dataset encoded with the VVC reference software encoder. Our proposal relying on the top-3 configuration reaches 46.6% complexity reduction for a negligible bitrate increase of 0.86%. A top-2 configuration enables a higher complexity reduction of 69.8% for 2.57% bitrate loss. These results emphasize a better trade-off between VTM intra coding efficiency and complexity reduction compared to the state-of-the-art solutions¹.

Index Terms—VVC, MTT, complexity reduction, CNN, DT.

I. INTRODUCTION

The emerging video formats such as 4K/8K and 360-degree videos alongside the explosion of IP video traffic [1] pushed organizations such as ISO/IEC, ITU-T Joint Video Expert Team (JVET) and Alliance for Open Media (AOM) to propose new video compression standards. AOM developed the AV1 codec released in 2018 as a successor to VP9 and JVET standardized Versatile Video Coding (VVC) ITU-T H.266 | MPEG-I - Part 3 (ISO/IEC 23090-3) [2] in July 2020 as a successor to High Efficiency Video Coding (HEVC).

These two standards share the same hybrid video coding structure. Therefore, during standardization different coding

tools were integrated to improve the intra and inter predictions, the in-loop filtering or to enhance the partitioning of the block of pixels. The selection of specific coding tools leads to different coding efficiencies and computational costs. Comparison studies were conducted between VVC and AV1 [3], [4] based on subjective and objective quality metrics including Peak Signal-to-Noise Ratio (PSNR) and Video Multi-method Assessment Fusion (VMAF) which is a Machine Learning (ML) based quality metric leveraging detail loss metric, visual information fidelity measure and averaged temporal frame difference. Both works conclude that VVC outperforms AV1 in terms of both objective and subjective quality scores. However, computational cost of AV1 fluctuates around the VVC complexity depending on the considered coding configuration.

The VVC reference software, named VVC Test Model (VTM), implements all normative VVC coding tools allowing rate-distortion-complexity evaluation and conformance testing. As the successor to HEVC, the VTM implementation brings 25.32% and 36.95% bitrate reductions at the expense of significant increases in encoder computational complexity estimated to 2630% and 859% compared to the HEVC test Model (HM) 16.22 [5] in All Intra (AI) and Random Access (RA) configurations, respectively.

Compared to HEVC, which is based on a Quad-Tree (QT) block partitioning, VVC integrates a nested Multi-Type Tree (MTT) partitioning scheme allowing in addition to QT, horizontal and vertical Binary-Tree (BT) and Ternary-Tree (TT) splits [6]. This new partitioning scheme is the most efficient tool integrated in VVC [7] with 8.5% coding efficiency gain reached in RA configuration compared to HEVC. Nevertheless, this coding efficiency improvement is brought at the expense of a significant complexity increase. At each level of the hierarchical partitioning process, up to five splits are tested by the encoder, compared to the one split (i.e. QT split) for HEVC. Authors in [8] have shown that disabling BT and TT splits, decreases the encoding time by 91.7%. Therefore, the partitioning process offers the highest opportunity in terms of complexity reduction compared to other coding tools. In [9], up to 97.5% complexity reduction was reported when only the optimal split is tested by the encoder at each level of the partitioning process compared to an exhaustive search.

To enable real-time VVC encoder, the complexity of the QT-MTT partitioning process must be significantly reduced. The aim of this work is to maximize the complexity reduction while minimizing the Bjøntegaard Delta Bit Rate (BD-BR) loss. A large body of literature has investigated the problem of block partitioning for HEVC [10], [11], [12] and VP9 [13]. For instance, Xu *et al.* [14] proposed a Convolutional Neural

A. Tissier, S. Belhadj Dit Mdalsi, W. Hamidouche and D. Menard are with INSA Rennes, Institute of Electronic and Telecommunication of Rennes (IETR), CNRS - UMR 6164, VAADER team, 20 Avenue des Buttes de Coesmes, 35708 Rennes, France. (emails: alexandre.tissier2@insa-rennes.fr, wamidou@insa-rennes.fr, and dmenard@insa-rennes.fr).

J. Vanne is with Tampere University, Korkeakoulunkatu 10, Tampere, 33720, Finland (emails: jarno.vanne@tuni.fi).

F. Galpin is with InterDigital, Cesson-Sévigné, 35051, France.

¹The source code of the proposed method and the training dataset will be made publicly available at https://alexandretissier.github.io/QTMTT_VVC/.

Network (CNN) to predict a hierarchical partition map in order to avoid exploring improbable block depths. However, such approaches cannot be directly applied to VVC as the new partitioning scheme is significantly different and more complex with the multiplication of available partitions which makes hard predicting the optimal block depth due to the huge number of partitions that can lead to the same depth. Recently, a number of complexity reduction methods tailored for VVC have emerged through fast encoder strategies [6], probabilistic approach [15] or machine learning based approach [16]. Deep learning techniques [17] provided a breakthrough in video coding and especially in the complexity reduction domain. Li *et al.* [17] proposed a CNN that predicts the most probable split through a multi classification at each block depth. One of the drawbacks of this technique is the time overhead due to the CNN inference performed at each depth. Indeed, the CNNs computational complexity must be managed in order to not annihilate the gain obtained by the complexity reduction technique. Authors in [18] have recently proposed a CNN that processes a block to predict its partition through a vector of probabilities. The average probability over edges of the split is then compared to a fixed threshold to decide whether to perform the split or not at each depth. The main drawbacks of this solution are first its local decision which does not leverage all probabilities of the block edges and second in comparing the average probability of the split edges to a fixed threshold.

In this paper, we propose an efficient complexity reduction technique for the QT-MTT partitioning. Our approach combines a moderate complexity CNN that extracts spatial features of the block of pixels with multi-class classifiers to derive the best partitions to evaluate in the Rate-Distortion Optimization (RDO) process. A single CNN is used to process a 64×64 block and predicts as output the probability of each boundary of all the 4×4 pixel blocks within the input 64×64 block. At each level of the hierarchical partitioning process, a multi-class classifier is used to predict from the set of boundary probabilities the N -most likely splits to explore by the encoder. One classifier is trained for each size of the 16 different sub-blocks. At each depth, the number of tested partitions N can be adjusted from one to the total number of possible splits. This allows exploring wide range of trade-offs between the complexity reduction and the quality loss. The proposed solution with top- $N = 3$ configuration reaches 46.6% complexity reduction for a negligible BD-BR increase of 0.86%. The top- $N = 2$ configuration enables in average a complexity reduction of 69.8% for 2.57% BD-BR loss.

The rest of this paper is organized as follows. Section II introduces the partitioning background and the state-of-the-art of complexity reduction techniques. Section III describes the proposed two-stage method based on the combination of two machine learning algorithms. The used dataset to train our models is detailed in Section IV. The experimental setup and the training processes for both CNN and Decision Tree (DT) models are presented in Section V. Section VI presents the performance of the two machine learning models and a comparison of our method against state-of-the-art techniques in terms of complexity reduction and BD-BR increase. Finally, Section VII concludes the paper.

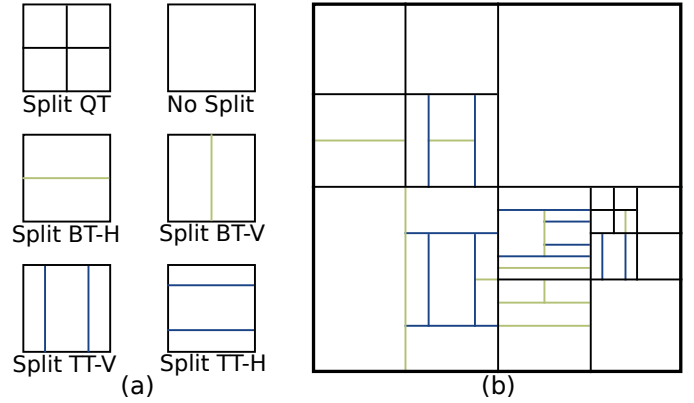


Fig. 1. CTU partitioning in VVC. (a) VVC split types. (b) Example of a CTU partition in MTT.

II. BACKGROUND AND RELATED WORK

A. Frame partitioning in Versatile Video Coding (VVC)

The new block partitioning scheme proposed in VVC is the most efficient coding tool integrated in the standard [19]. The partitioning starts the process on a root block named Coding Tree Unit (CTU), i.e. a block of 128×128 pixels in the VVC Test Model (VTM) All Intra (AI) configuration. The blocks resulting from the partitioning process are named Coding Units (CUs) and may have a size between 64×64 and 4×4 . Fig. 1(a) presents the splits supported by VVC. As High Efficiency Video Coding (HEVC), Quad-Tree (QT) divides a CU in four equal sub-CUs. Moreover, VVC allows rectangular shape for CU with its novel splits Binary-Tree (BT) and Ternary-Tree (TT). The BT divides a CU in two sub-CUs while the TT divides a CU in three sub-CUs with the ratio 1:2:1. Both BT and TT can split a CU horizontally or vertically. Fig. 1(b) presents the splits of a CTU processed by VTM Rate-Distortion Optimization (RDO). The RDO process relies on an exhaustive search that calculates the Rate-Distortion (RD)-cost for each CU and selects the CTU partition that results in the lowest RD-cost. In AI configuration, the VTM forces the first split of the CTU to be a QT. Additional constraints are also applied on CUs, for instance, QT is not allowed after a BT or a TT split. Excluding the VTM restrictions, the encoder performs all possible splits on each CU in order to select the optimal partition with the lowest RD-cost.

B. Existing techniques for encoder complexity reduction

A brief review on complexity reduction methods proposed to speedup the reference software encoders of the HEVC and VVC standards is provided in this section. Authors in [9] have studied the complexity reduction opportunities in the VTM3.0 under the AI configuration. Several tools have been identified to reduce the encoding complexity such as the partitioning process, the intra mode prediction and the multiple transform selection. This study showed that the partitioning process has the highest impact on encoder computational complexity with 97.5% of complexity reduction followed by the intra mode prediction with 65.2% and the multiple transform selection

with 55.2%. This study motivated the work of this paper that tackles the complexity reduction of the partitioning process.

Meanwhile, several works have studied the complexity reduction of the intra mode prediction [20] and the multiple transform selection [21]. In order to reduce the complexity of the partitioning process, state-of-the-art solutions rely on different approaches to compute features relevant for this problem including handcrafted and learning-based techniques. The computed features are then fed to a classifier such as Decision Tree (DT), Support Vector Machine (SVM) or dense layers. It should be noted that the performance of the most following techniques is provided under the AI coding configuration unless otherwise specified.

1) *HEVC complexity reduction techniques*: The complexity reduction of the HEVC recursive block partitioning has been widely investigated in the literature. Min *et al.* [22] defined a complexity score metric that predicts the spacial complexity of a block. The complexity score is computed as the l_1 norm of the differences between the luminance pixel value at a position and the mean luminance value. This complexity score is computed for the two sub-blocks obtained by dividing the block in horizontal, vertical or in the two diagonals. The difference between the two complexity values of the resulting sub-blocks is computed. This value is then compared to a predefined threshold to decide whether the block should be split, no split or undetermined. This solution reaches 52% of complexity reduction at the expense of a slight Bjøntegaard Delta Bit Rate (BD-BR) increase of 0.8%. Correa *et al.* [10] used three sets of decision tree trained with features such as RD-cost, gradient, sum of pixels or variance of pixels. These decision trees predict whether the CU, Prediction Unit (PU) or Transform Unit (TU) must be split or not. By predicting these partitioning specific to HEVC, this solution achieves 65% of computational complexity reduction for 1.36% BD-BR loss. Convolutional Neural Networks (CNNs) have already been exploited for HEVC encoding complexity reduction [14], [11]. Xu *et al.* [14] first used a CNN to predict a hierarchical CU partition map which provides an efficient representation of the CU partitioning in intra mode. An Long-Short Term Memory (LSTM) network was then integrated to predict the partition in inter prediction mode. In AI configuration, this solution reduces the complexity by 62% for 2.25% BD-BR increase. Under the low delay P coding configuration, it reaches 54.2% of computational complexity reduction for 1.5% BD-BR increase. Li *et al.* [11] claimed a real time CTU partition prediction based on their previous proposed complexity reduction method presented in [14]. They simplified the CNN by pruning the weights at different levels to perform multiple approximations. These different configurations allow a complexity control at CTU level by selecting the proper CNN. An estimation of the CNN run time is performed at the frame level to enhance the stability of complexity control. The CNN run time speedup is enhanced by 17 to 20 times with a complexity control error of 2%.

2) *Joint Exploration Model (JEM) complexity reduction techniques*: The JEM software was developed in early 2014 to study the potential coding gain behind developing a new standard beyond HEVC. The JEM software is based on HEVC

test Model (HM) with new coding tools such as Multiple Transform Selection (MTS) and BT proposed to enhance the partitioning efficiency at the cost of higher computational complexity. Wang *et al.* [15] proposed a novel RD-cost estimation scheme relying on motion divergence field. Based on the estimated RD-cost, a probabilistic framework is developed to skip unnecessary splits. The proposed algorithm reduces the complexity by 54.7% for 1.15% BD-BR increase in Random Access (RA) configuration. The same authors proposed in [23] as first step a dynamic parameters choice at CTU level based on neighboring partitions. In a second step, both QT and BT decision tree classifiers predict the probability of the different splits in order to derive the proper partition. These two techniques enable 67.6% of complexity reduction for 1.34% BD-BR increase in AI configuration. Jin *et al.* [24] designed a multi-classification CNN that predicts the partition depth of a 32×32 CU. This method enables skipping unnecessary splits for the partition depth predicted as outside the candidate depth range. The encoder computational complexity is reduced by 42.8% for a BD-BR increase of 0.65%.

3) *VVC complexity reduction techniques*: Even-though VVC was recently standardized, several techniques have been already proposed to tackle the problem of encoder complexity. Indeed, the extension of the partitioning process with QT, BT and TT splits considerably increases the encoding computational time. Predicting a split at each CU becomes a real challenge due to the number of partition possibilities that have increased significantly compared to HEVC. This situation raises the need for lightweight partitioning process that decreases the encoder complexity while preserving its coding efficiency for live applications. Fu *et al.* [25] proposed a block partitioning algorithm through a Bayesian decision. This technique explores information of previously tested BTH to skip vertical splits. The TTH split can also be early skip relying on the BT information and specifically the difference between the RD-cost of BT splits. This technique reaches 44.8% of computational complexity reduction for 1.02% BD-BR increase. Lei *et al.* [29] proposed a two-step look-ahead prediction method for the intra prediction mode and partitioning process. This solution computes the rate-distortion cost of only 7 intra modes out of 67 and if a CU has multiple partitions, the RD-cost of partitioned CU are computed from the parent CU. Moreover, this solution approximates the RD-costs of different partition directions in order to skip unnecessary directions. Intra mode technique combined with partitioning prediction technique allows a computational complexity reduction of 45.8% for 1.03% BD-BR increase. Amestoy *et al.* [16] proposed a cascade framework through random forest classifiers to determine the probability of each split. In order to improve the accuracy of their classifiers, the impact of each feature is evaluated such as Quantization Parameter (QP), variance and mean of the block gradients. Furthermore, the thresholds applied to the different classifiers are optimized. A risk interval was proposed to limit the RD-cost increase by computing both splits of the classifier output when the probability falls in this risk interval. In RA configuration, this solution enables from 30.1% to 61.5% of complexity reduction for respectively 0.61% to 2.22% BD-BR increase depending

TABLE I
MAIN FEATURES OF EXISTING STATE-OF-THE-ART COMPLEXITY REDUCTION TECHNIQUES IN ALL INTRA CODING CONFIGURATION.

Solution	Handcrafted	Decision Tree	Neural network	Software	Complexity reduction (%)	BD-BR (%)
Biao <i>et al.</i> [22]	✓	✗	✗	HM 10.0	52%	0.8%
Xu <i>et al.</i> [14]	✗	✗	✓	HM 16.5	62%	2.25%
Wang <i>et al.</i> [23]	✓	✓	✗	HM 13.0 QTBT	67.6%	1.34%
Jin <i>et al.</i> [24]	✗	✗	✓	JEM 3.1	42.8%	0.65%
Fu <i>et al.</i> [25]	✓	✗	✗	VTM 1.0	44.8%	1.02%
Yang <i>et al.</i> [26]	✓	✓	✗	VTM 2.0	52%	1.59%
Chen <i>et al.</i> [27]	✓	✓	✗	VTM 4.0	51.2%	1.62%
Li <i>et al.</i> [17]	✗	✗	✓	VTM 7.0	45.8%	1.32%
Zhao <i>et al.</i> [28]	✓	✗	✓	VTM 7.0	39.4%	0.87%

on the risk interval configuration. Another cascade framework was proposed by Yang *et al.* [26] with one binary classifier for each split mode. The authors used three categories of features including global texture information, local texture information and context information as input of their classifiers. A fast intra mode decision using one dimensional gradient descent search is combined with the CTU structure decision. This fast partitioning solution achieves 52% of complexity reduction for 1.59% BD-BR increase. The intra mode decision technique enhances the complexity reduction to 62.5% for 1.93% BD-BR loss. Chen *et al.* [27] also used a supervised learning method. Instead of a cascade framework, they designed six SVM models depending on the CU sizes which are trained to skipped vertical and horizontal splits. SVM features are derived from entropy, texture contrast and Haar wavelet of the current CU. This solution reaches 51.2% of computational complexity reduction for 1.62% BD-BR increase. Li *et al.* [17] proposed a deep learning approach to predict the CTU partition with a binary or multi classification at each CU depth. To train the CNN, they designed an adaptive loss function that defines penalty weights based on split proportion that penalizes high difference between the RD-cost for the split predicted and the minimum RD-cost of the parent CU. Based on the prediction accuracy of the CU size, an adaptive threshold is compared to the output of the CNN. This technique enables to reduce the complexity by 45.8% for 1.32% BD-BR increase. Another CNN model is proposed by Zhao *et al.* in [28]. First, the standard deviation of CU pixels is compared to an adaptive threshold based on QP and CU depth in order to classify a block into complex or homogeneous CU. The CU defined as homogeneous are no more split. Second, for complex CU, a CNN is trained to predict whether the current CU must be early terminated or not. This solution achieves 39.4% of computational complexity reduction for 0.87% BD-BR increase.

Table I summarizes the features and performance of the aforementioned VVC complexity reduction techniques. It can be noticed that different techniques rely on artificial neural network especially CNN. Those techniques are showing outstanding performance compared to other state-of-the-art techniques.

III. PROPOSED TWO-STAGE VVC PARTITION PREDICTION SOLUTION

As described in Section I, VVC introduces BT and TT splits at the cost of a high increase in computational complexity. This recursive partitioning process computes the rate-distortion cost for a set of coding tools for each CU. The proposed partitioning prediction technique is composed of a CNN for spatial features extraction followed by a set of multi-class classifiers based on DTs to predict the appropriate partitioning decision at different depths of the partitioning tree. Fig. 2 illustrates the flow diagram of the proposed partitioning prediction solution.

A. Overall presentation

Our method is a top-down solution that early terminates unlikely splits, i.e. it follows the hierarchical process of the VVC encoder and skips split that have a low probability to belong to the optimal partitioning. Our complexity reduction method is composed of two components including spatial features extraction and DT classifiers. The features extraction block consists of a CNN that processes an input luminance block \mathbf{B} to predict a vector of probabilities $\tilde{\mathbf{p}}$ of splits at the 4×4 block edges:

$$\tilde{\mathbf{p}} = f_{\theta}(\mathbf{B}). \quad (1)$$

where f_{θ} is a parametric function of the CNN with trainable parameters θ and \mathbf{B} is the input block of size 68×68 .

The block \mathbf{B} consists of the current CU of size 64×64 padded with four rows and four columns on the top and left of the block resulting in a block size of 68×68 . The left and top neighbor pixels are used as reference samples in the intra prediction through the Multiple Reference Line (MRL) intra prediction [30]. Indeed, their pixels are used to derive the intra mode of the current block. Therefore, it is important to include these samples in the features extraction stage. The CNN predicts for each $N_B \times N_B$ CU a vector of N_p probabilities of a split at each 4×4 edge of the block. The length N_p of the predicted probabilities vector $\tilde{\mathbf{p}}$ is computed as follows:

$$N_p = \frac{N_B}{2} \left(\frac{N_B}{4} - 1 \right). \quad (2)$$

In the case of CU size of 64×64 , N_p is the length of the vector $\tilde{\mathbf{p}}$ which is equal to 480. Fig. 3 presents the connections between the probability vector components and the 480×4 edges of an input CU. As highlighted in this figure, the

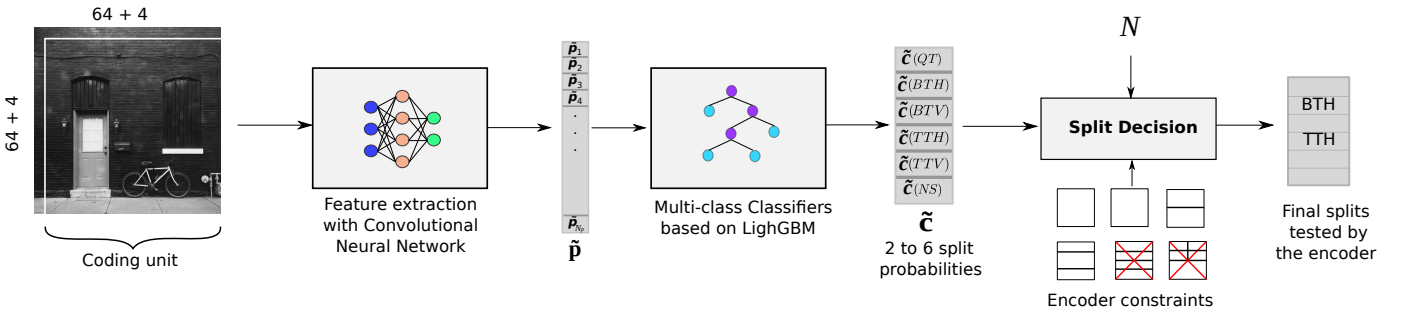


Fig. 2. Workflow diagram of the proposed block partitioning scheme for VVC AI coding. The input luminance block is first processed by a CNN to predict $\hat{\mathbf{p}}$, a vector of N_p probabilities describing all edges at each 4×4 sub-block. The vector $\hat{\mathbf{p}}$ is then processed by a decision tree LightGBM to predict probabilities of the six partitioning options through the vector $\tilde{\mathbf{c}}$. The top- N splits of the highest probabilities are tested by the RD process of the encoder to select the optimal split in terms of RD-cost.

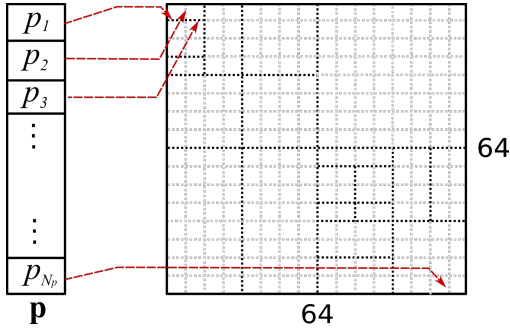


Fig. 3. Correspondence between the CNN output vector and a 64×64 CU partition.

first p_1 and the third p_3 components of the vector correspond to the bottom horizontal edges of the first and second 4×4 blocks, respectively. For a good partitioning prediction, these two components must have a value (probability) close to 1 as a TT split is performed to split the sub-block. The last component of the vector p_{N_p} has a value (probability) close to 0 since no split is performed at this last vertical edge of the CU as illustrated in Fig. 3.

The classifiers are then fed with the probabilities vector $\hat{\mathbf{p}}$ derived from the CNN to predict the split decision to perform at each tree depth

$$\tilde{\mathbf{c}} = g_{\omega_i}(\hat{\mathbf{p}}), \quad \forall i \in \{1, \dots, M\}, \quad (3)$$

where g_{ω_i} is a parametric function of a classifier i , ω_i is its trainable parameters and M is the number of considered classifiers.

A separate multi-class classifier based on DT model is applied for each CU size. The classifier takes as input the probability vector $\hat{\mathbf{p}}$ and predict a vector $\tilde{\mathbf{c}}$ of six probabilities that correspond to the six possible splits performed by the VVC encoder at each tree depth. This approach results in M separate DT models that are trained separately to enhance the prediction performance and enable better convergence of the model with reduced number of trainable parameters. Once the split probabilities are derived for the CU, a selection of the highest probabilities is made based on the selected configuration. The configuration specifies the N value which defines the number of tested splits by the encoder. Thus,

the encoder performs only the N first splits corresponding to the highest probabilities (Top- N) predicted by the DT model. The remaining splits with lower probabilities than the top- N candidates are skipped by the encoder to reduce the encoding computational complexity. The proposed spatial features extraction CNN model and the DT classifiers are described in more detail in the next two sections, respectively.

B. Spatial features extraction CNN model

Fig. 4 presents the adopted CNN architecture which is inspired by the ResNet network [31]. The orange layers represent convolution layers with 3×3 kernel (Conv 3×3), whereas the yellow layers denote convolutions with 1×1 kernel (Conv 1×1) that transform the input feature map matrix to match the dimension of next layer which are then summed up (green plus). The red layers correspond to the max pooling (Max Pool) that subsample the input features map with a window of 2×2 by selecting the maximum over four values. The last layer in purple is a fully connected layer (Dense) that predicts the 480 components vector. The sigmoid activation function is used to predict the output values within the interval $[0, 1]$. All these layers result in a network with 226,088 trainable parameters. The input consists of a 68×68 luminance pixels of the CU currently processed plus the QP value that highly influences the final partition. The QP is provided as an external input to the last fully connected layer. The QP parameter is crucial to save the memory bandwidth as it leads to only one model shared for all QP values instead of adopting one model by QP value. Therefore, our model can be efficiently used with a rate control mechanism that adapts the QP value to the target bandwidth. The output is a 480 components vector that represents the fine-grain partitions (4×4) of the 64×64 CU. This solution has the advantage of predicting the whole CU spatial features in one shot, which is very convenient to reduce the complexity overhead and latency introduced by this step. Moreover, the architecture of the network is less deep than state-of-the-art CNN architectures [32], [33] and thus will require less time to predict the output vector.

C. Multi-class classifiers based on DT models

The decision approach adopted in our previous work [18] relied only on the probability at the spatial location of a

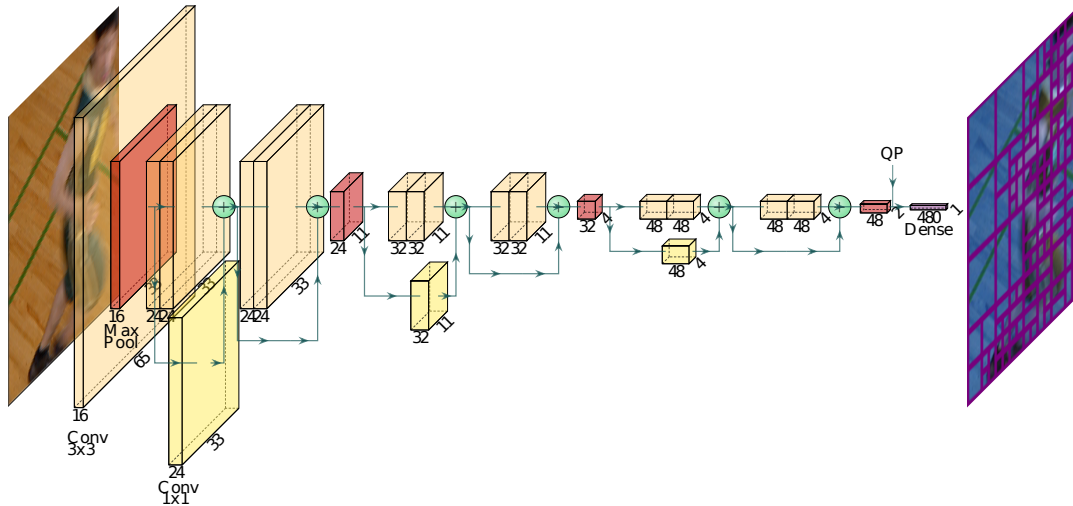


Fig. 4. The CNN architecture with convolution layers in orange and yellow, max-pooling layers in red and fully connected layer in purple.

specific split. For instance, the BTH split takes into account only the probabilities of the horizontal edges in the middle of the CU. By leveraging only a restricted location of the CU, an important information is omitted to determine the final split decision. In order to take advantage of all probabilities inside the current CU, the DT model is adopted to process the vector of probabilities predicted by the CNN model. This vector of probabilities can be considered as spatial features relevant for the block partitioning process. Therefore, the CNN inference is carried-out once for each CU of size 64×64 to predict the corresponding probability vector \mathbf{p} , and then a specific DT model processes this vector at each level of the partitioning tree to derive a set of N more likely splits to explore by the encoder. To predict split probabilities at various CU sizes, multiple models are considered covering all possible sizes of the rectangular sub-blocks from 64×64 to 4×4 excluded. As illustrated in Table II, sixteen CU sizes can be further split in six to two different partitions including the no split option. The DT model is fed with the probability vector $\tilde{\mathbf{p}}$ and the QP value. The probability vector is then cropped into a sub-vector that includes only the probabilities of the sub-block edges. The DT model performs a multi-class classification by predicting a probability vector $\tilde{\mathbf{c}}$ of six components corresponding to the probabilities of the six possible splits. Therefore, the probabilities of non possible splits are set to zero during the training process.

Several machine learning models have been investigated to solve this multi-class classification problem including DT, random forest, SVM with different kernels and Light Gradient Boosting Machine (LGBM) model [34]. This latter has been retained for its good classification performance associated with low complexity at both training and inference stages.

IV. PROPOSED DATASET FOR TRAINING

In this section, first, our dataset is presented through its representations. Second, the process to balance the dataset is detailed for both soft and hard representations.

TABLE II
POSSIBLE SPLITS ACCORDING TO THE CU SIZE

Width \ Height	64	32	16	8	4
64	QT	-			
32	-	All	BT, TT	BT	BTH
16		BT, TT	All	TTH	TTH
8		BT, TTV		BT	BTH
4		BTV, TTV		BTV	-

TABLE III
BREAKDOWN OF OUR DATASET BY RESOLUTION.

Resolution	240p	480p	720p	1080p	4K	8K	Total
Nb images	500	500	579	2557	654	418	5208

A. Dataset for the learning process

The lack of public dataset providing encoded blocks with the VTM and their corresponding partitions drives us to construct our training dataset to optimize the proposed models weights. As our work focuses on AI configuration, temporal relationship between frames is not considered. Therefore, five public image datasets were selected including Div2k [35], 4K images [36], jpeg-ai [37], HDR google [38] and flickr2k [39]. The resulting dataset presents a high diversity of still image contents. However, since these datasets include more images in high resolution (Full HD and 4K resolutions), a set of high resolution images downsampled with a bilinear filter are added to the dataset. This results in a dataset with around 5208 images at different resolutions as detailed in Table III which gives the number of images per resolution. The images of the same resolution are then concatenated to build a pseudo-video sequence. This latter is encoded with the VTM encoder in AI configuration at different QP values, QPs $\in \{22, 27, 32, 37\}$.

It should be noticed that the VTM encoder includes multiple speed-up techniques for the partitioning process to overcome the complexity brought by the VVC partitioning process [6]. To achieve a high coding efficiency by testing more partitioning configurations, these speedup techniques have been

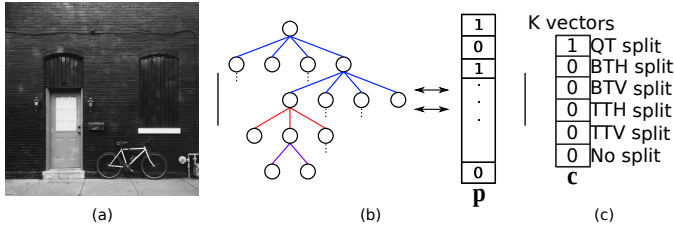


Fig. 5. Representation of our dataset. (a) is a luminance 68×68 input block **B**. (b) is the optimal partitioning of the block represented by a tree and transformed to the soft representation, i.e. a 480 elements vector \mathbf{p} . (c) is the hard representation, K vectors \mathbf{c} of 6 probabilities, that define the optimal split for each of the K blocks in the tree. K is the decision tree depth.

disabled to build our dataset. Compared to the VTM anchor, disabling these speed-up techniques enhances the coding efficiency with more accurate partitioning configurations. Nevertheless, a higher encoding time is needed to create the ground truth but only one encoding pass is required, so, increasing the encoding time is not critical at this stage. The VTM in AI configuration relies on the dual tree tool that performs separate partitioning for luminance and chrominance components. The partitioning information of both components is recorded while only the prediction of luminance partitioning is considered in this paper since it takes the most part of the encoding complexity with more than 85% of the total encoding time [8].

The optimal partitions computed by the VTM encoder is first saved as a tree. Therefore, in order to integrate the dataset in our proposed method, two data representations are defined as soft and hard representations as illustrated in Fig. 5. Fig. 5-(a) shows a block **B** processed by the VTM encoder which is a 64×64 luminance block plus 4 rows and columns on top and left of the block. These supplementary pixels are required for the MRL intra prediction tool. Fig. 5-(b) illustrates the partition tree of the this block which is converted to a 480 components vector. This soft representation of the tree depicts the 64×64 block luminance partition in 4×4 blocks in a single vector \mathbf{p} . The hard representation of our dataset is a succession of K vectors that defines all splits at each depth. Fig. 5-(c) presents one of those vector \mathbf{c} which defines the optimal split for a specific CU size. The vector size is set to six as the maximum number of splits defined by VVC. For instance, the 64×64 CU size has only two possible splits with QT and no split and thus the rest of four vector components are set to zero. Instead, for a CU size of 32×32 , all splits are available, so the vector size is 6 with QT, the two BTs, the two TTs and no split.

B. Dataset processing

Our dataset includes more than 26 million instances of 64×64 block partition excluding any Common Test Conditions (CTC) sequence to insure a fair comparison of our method against state-of-the-art techniques. In order to analyze the dataset disparity, a first selection of 2 million instances are picked randomly. Furthermore, to address the data heterogeneity issue of the dataset, several classes are defined with 8 levels of depth partition from no partition to deep partition. Fig. 6 gives the number of instances in the dataset at each of

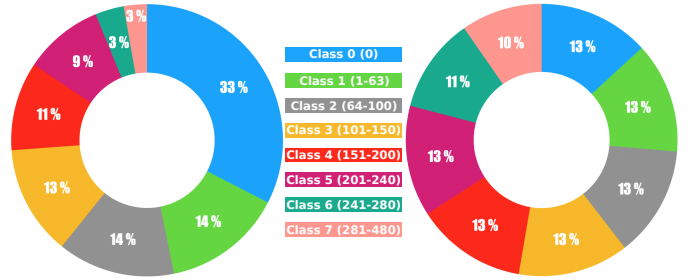


Fig. 6. Breakdown of our dataset by partition classes. (a) Unbalanced dataset. (b) Balanced dataset.

these 8 depth levels which are defined based on the number of edges activated in the 64×64 CUs. Fig. 6-(a) represents the class repetitions through 2 million instances before the dataset balancing. It can be noticed that the class 0 without any split contains more than a third of the 2 million 64×64 CUs instances, while the last two classes which illustrate deep partition are under-represented and must therefore be increased. Fig. 6-(b) illustrates the depth distribution of block partitioning over the eight classes after the dataset balancing. 1,200,000 instances (64×64 block) were selected at each QP value with a homogeneous representation over the eight classes. The two last classes are slightly under-represented as highly deep partitions are derived by the encoder only for extremely complex blocks encoded at low QP values.

The hard representation is composed of sub-datasets separated by the different CU sizes. These sub-datasets are also balanced to enhance their representation. Indeed, we balanced individually each sub-dataset over the available splits and the QPs. For instance, the 4×16 CU size dataset is balanced between the proportion of BTH, TTH and no split but also among the 4 QPs.

V. TRAINING PROCESS AND EXPERIMENTAL SETUP

A. CNN model

The CNN is trained from scratch with the proposed dataset described in Section IV relying on the Keras framework [40] running on top of Tensorflow module [41]. The weights θ of the CNN are updated at each batch iteration with the ADAM stochastic gradient descent optimizer [42]. The loss function is defined to optimize those weights by minimizing the mean squared error between the predicted probability vector $\tilde{\mathbf{p}}$ and the corresponding ground truth vector \mathbf{p} as follows:

$$\mathcal{L}_{cnn} = \|\mathbf{p} - \tilde{\mathbf{p}}\|_2^2. \quad (4)$$

The batch size is set to 128 instances (64×64 CUs) and the learning rate is equal to 10^{-3} .

A hundred epochs are processed with a random shuffle of the dataset at each epoch. The CNN training was carried out on a RTX 2080 Ti Graphics Processing Unit (GPU).

B. DT LGBM model

The DT models are implemented under the LGBM framework [34] version 2.3.1. This latter is a gradient boosting framework based on decision tree developed by Microsoft.

LGBM has many advantages such as its low memory usage, the capacity of handling large-scale data and the low inference computational time. This last advantage is essential for our problem as the inference is carried-out at each CU level.

LGBM is a DT method that sums the predictions of all the trees to get a richer interpretation of the problem. The trees are optimized in a stage-wise way by adding or updating one tree sequentially based on the error of the whole ensemble learned so far. For DT classification, the loss function is defined as follows

$$\mathcal{L}_{dt} = - \sum_{i=1}^6 c_i \log \tilde{c}_i, \quad (5)$$

where c_i is the vector of ground truth split probabilities and \tilde{c}_i is the vector of split probabilities predicted by the model.

C. Evaluation procedure and implementation details

All experiments are conducted with the VVC Test Model (VTM) version 10.2 in AI coding configuration. We consider test video sequences defined in the VVC Common Test Conditions (CTC) [43]. The CTC video sequences are separated in seven classes as follows: A1 (3840×2160), A2 (3840×2160), B (1920×1080), C (832×480), D (416×240), E (1280×720), and F (832×480 to 1920×1080). These video sequences are encoded at four QP values: 22, 27, 32 and 37.

The proposed solution is assessed in terms of both coding efficiency and computational complexity. The coding efficiency is measured with the BD-BR metric [44] that measures the bitrate loss over four QPs in percentage with respect to the anchor (ie. VTM10.2) for the same Peak Signal-to-Noise Ratio (PSNR) objective quality. The computational complexity reduction with respect to the anchor is assessed by computing the Δ Encoding Time (ΔET) as follows:

$$\Delta ET = \frac{1}{4} \sum_{QP_i \in \{22, 27, 32, 37\}} \frac{T_R(QP_i) - T_C(QP_i)}{T_R(QP_i)}, \quad (6)$$

where T_R is the reference encoding time of the VTM anchor and T_C is the encoding time of the VTM with the proposed complexity reduction method.

Our complexity reduction technique has been integrated in the VTM10.2 encoder which is developed in C++ programming language. The CNN is built and trained with Python under the Keras framework and then the model is converted to C++ code with the frugally deep framework [45]. The DT models are also trained in python and then converted to C++ with the LGBM framework [34].

All encoding operations were carried out sequentially on an Intel Xeon E5-2603 v4 processor running at 1.70 GHz under Ubuntu 16.04.5 operating system (OS).

VI. EXPERIMENTAL RESULTS

In this section the performance of the proposed method is assessed. The CNN performance is analyzed through its accuracy and Receiver Operating Characteristic (ROC) curves. The multi-class DT classifiers accuracy is presented through its top-N accuracy. The complexity reduction proposed method is then assessed in terms of both computational complexity

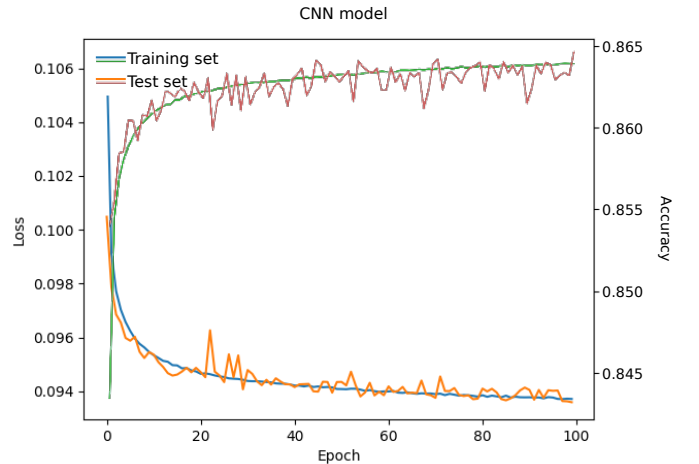


Fig. 7. Decreasing loss (in X) and increasing accuracy (in Y) as a function of epoch for the training and test set.

reduction and BD-BR increase with respect to the VTM. Multiple configurations of our method are explored depending on the tested top-N DT LGBM output splits. There are several existing techniques that have investigated the complexity reduction induced by the new MTT partitioning in VVC. The proposed solution is compared with four best performing state-of-the-art techniques including solutions proposed by Fu *et al.* [25], Chen *et al.* [27], Yang *et al.* [26] and Li *et al.* [17]. Finally, the inference overheads of both CNN and DT models are assessed.

A. CNN performance

Fig. 7 shows the loss and accuracy of the CNN model versus the training epochs on both training and test datasets. The blue and orange decreasing curves correspond to the losses computed by Eq. (4) over hundred of epochs of the training. The green and red increasing curves represent the binary accuracy computed after a shrinkage with a threshold of 0.5. It means that if a predicted value is higher or lower than 0.5, the value is considered to be 1 or 0, respectively. This resulting value is compared to the ground truth and the accuracy is computed over all components of the vector of probabilities. The two curves in blue and green are from the training part and those in orange and red are from the testing part. The goal of the training is to update the model weights to minimize the loss at each iteration. We can notice that the loss curves decrease from 0.105 to 0.094 over 100 epochs for both training or test datasets. The test curve follows the training one which means that the model generalizes well on the test set. The model accuracy reaches more than 86% of good prediction, i.e. 86% of the estimated probabilities with a threshold of 0.5 are equal to the ground truth.

The CNN prediction performance is also analyzed under VTM with the ROC curves. The ROC curves represent the true positive rate versus the false positive rate. These curves select a target split to analyze versus all the other possible splits. The split probabilities required to plot these ROCs are

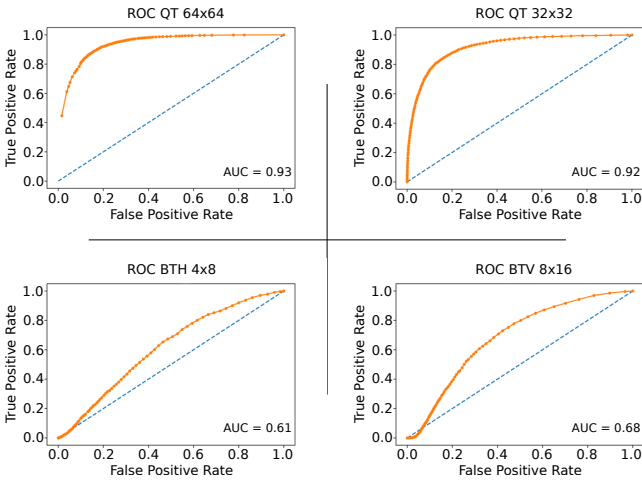


Fig. 8. Several CNN ROCs for different splits and sizes on the CTC video sequences.

determined by averaging all probabilities which are at the exact spatial position of the split. Fig. 8 presents the ROC curves of QT, BTH and BTV splits at different CU sizes computed on the CTC sequences. The QT ROC curves show that the average probability is able to reach 0.8 of true positive for approximately 0.1 of false positive rate, for both 64×64 and 32×32 CU sizes. Instead, the BT ROC curves are closer to the random guess curve which is the diagonal one in blue. Indeed, the CNN pays more attention to those probabilities. Moreover, the high CU sizes determine more easily the split choice as it concerns more pixels. The ROC area under curve value are given as a single score to compare the results among the graphs. As shown by the curves, the ROC area under curve confirms the results by reaching scores higher than 0.9 for the QT and less than 0.7 for the BT splits.

Visual illustrations of partitions of a 64×64 CU from ground truth and predicted by the proposed CNN are given on the first and second rows of Fig. 9, respectively. On the top row, the optimal partitions derived by the VTM anchor considered here as the ground truth. On the bottom row, the partitions predicted by the CNN are displayed with color codes based on their probabilities. The color code varies from red to blue with a probability ranging between 0.3 and 1 and gray color for probabilities below 0.3. The partitions for QP 37 is shallow with a maximum of three depths and two CUs of size 32×32 . Its CNN prediction is relevant with each edge defined as a split with a probability higher than 0.9. For the other edges that are not defined as a split, the probability are lower than 0.3 except six edges predicted with probabilities between 0.3 and 0.4. Compared to the QP 37 partition, the QP 27 configuration is partitioned deeper and is harder to predict efficiently. The figure shows that each edge determined as a split have a probability higher to 0.3 except the TT split and some CUs are predicted deeper.

It should be noticed that the CNN output is not directly used in the VTM. The CNN output is considered as spatial features and it is used as an input for the DT LGBM models. The DT LGBM will benefit from all the probabilities that have an impact on the CU partition.

B. DT LGBM performance

The second part of the proposed solution includes DT LGBM models that take advantage of all spatial features predicted by the CNN to derive split probabilities. As presented in Section IV, multiple models are trained to handle the different CU sizes. The input element ranges start from one probability plus the QP for 4×8 or 8×4 CU sizes to 480 probabilities plus the QP for 64×64 CU size. The output is a vector of six classes with QT, the two BTs, the two TTs and no split. For CUs with less splits available due to VTM restrictions, a mask is applied on the predicted vector to restrict the unsuited splits.

Table IV presents the accuracy of the DT LGBM models on CTC test set. Three values are reported to analyze the DT LGBM results based on the top-N accuracy with $N \in \{1, 2, 3\}$. top-N accuracy is a metric that measures how often the correct class falls in the top-N highest predicted probabilities. top-1 accuracy reaches in average 67.24% of correct prediction. Based on the number of the output classes the prediction is different. It decreases in average from 86.7% to 55.45% for 2 classes and 6 classes, respectively. The highest top-1 accuracy is achieved with the 64×64 CU binary classification between QT and no split with 91.69%. All DT LGBM models have more than 50% top-1 accuracy even with multi classification. The top-2 accuracy is presented for models with at least three classes, which reach in average 82.97%. The lowest accuracy is 71.27% obtained with the lowest CU size available for six classes decision, i.e. 16×16 . Finally, top-3 accuracy achieves 91.19% accuracy in average over the model with at least four classes. By skipping half of the available splits, the top-3 configuration achieves 86.74% accuracy for 6 classes. This enables to reduce the complexity by a factor of two with a high confidence on the prediction. These results exhibit that the accuracy of DT models with 3 classes depends on the available split. In fact, higher accuracy is reached for the 8×8 CU size model in top-1 and top-2 by at least +12% and +3% respectively compared to other models with 3 classes. In addition to the no split mode, two splits are in competition: either BT and TT in the same direction or BT horizontal and vertical. As shown by the results, the direction of a split is easier to predict than the difference between BT and TT in the same direction.

C. Complexity reduction performance under the VTM

The two-stage proposed model is integrated in the VTM10.2 AI encoder. For fair comparison, the reference used to compute the BD-BR loss and the complexity reduction is the VTM encoder including multiple native speed-up techniques [6] for the partitioning process. These speed-up techniques reduce significantly the execution time with a slight BD-BR degradation compared to an exhaustive RDO process. Thus, these experiments exhibit the gain provided by our approach compared to the common configuration of the VTM encoder.

To compare our method, the best performing state-of-the-art techniques in terms of complexity reduction and BD-BR loss metric are selected. These state-of-the-art techniques are not performed under the same VTM version, however, the

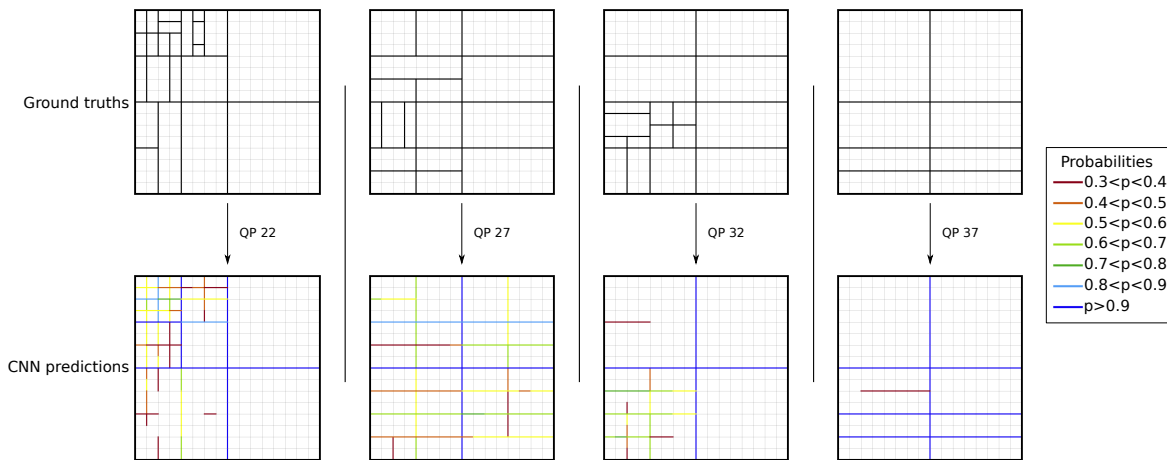


Fig. 9. Example illustration of ground truth partitions and the corresponding CNN predictions for the sequence MarketPlace with QPs 22, 27, 32 and 37.

TABLE IV
PERFORMANCE OF EVERY DT LGBM MODELS WITH THEIR DEFINED SIZE AND NUMBER OF OUTPUT THROUGH TOP-1, TOP-2 AND TOP-3 ACCURACY ON THE TEST SET.

Width	Height	Number of classes	Top-1 accuracy (%)	Top-2 accuracy (%)	Top-3 accuracy (%)
64	64	2	91.69	-	-
32	32	6	59.94	78.38	88.87
32	16	5	58.50	77.96	89.85
16	32	5	56.55	77.48	89.24
32	8	4	54.80	80.22	94.11
8	32	4	54.91	80.45	94.40
32	4	3	66.64	87.80	-
4	32	3	68.80	87.38	-
16	16	6	50.95	71.27	84.60
16	8	4	62.89	82.74	94.05
8	16	4	62.36	83.25	94.39
16	4	3	68.96	90.12	-
4	16	3	68.95	88.54	-
8	8	3	81.46	93.05	-
8	4	2	82.16	-	-
4	8	2	86.26	-	-
Average		2	86.70	-	-
		3	70.96	89.38	-
		4	58.74	81.67	94.24
		5	57.53	77.72	89.55
		6	55.45	74.83	86.74
	-	-	67.24	82.97	91.19

CTU partitioning tools have not been changed during the standardization.

Table V presents the BD-BR and complexity reduction performance of our method compared to the state-of-the-art techniques [25], [27] and [17]. In this table, two configurations are presented based on the top-2 and top-3 configurations. The results are illustrated for the CTC sequences from class A1 to class F. The average is presented for each class independently and for all the sequences from class A1 to class E. Class F is not taken into account for the average as it includes specific sequences such as screen content.

In average, through all the sequences our top-3 configuration reaches 0.86% BD-BR increase for a complexity reduction of 46.6%. Compared to Fu *et al.* [25] and Li *et al.* [17], our solution achieves better performance in terms of both BD-BR and complexity reduction. Chen *et al.* [27] solution reduces the complexity by 4.6% at the expense of significant increase of 0.76% in BD-BR compared to our top-3 configuration. This

low gain in the complexity reduction is not relevant compared to the increase in BD-BR which is almost doubled. The second configuration with top-2 achieves in average 2.57% BD-BR increase with 69.8% of complexity reduction.

High video resolutions are the main interest in VVC development. In fact, tackling high resolution complexity is particularly important as the encoding time is proportional to the sequence resolution. Both A and B classes represent high resolution sequences with 4K and full HD, respectively. Our top-3 and top-2 configurations are able to reach 47% and 66.6% complexity reductions for 0.7% and 1.85% BD-BR losses on class A sequences, respectively. In both BD-BR and complexity reduction metrics our method is better than Chen *et al.* [27] and Li *et al.* [17] techniques. Compared to these two techniques, our top-3 configuration solution achieves in average enhancements of 0.69% and 0.85% in BD-BR and computational complexity reductions of 1.5% and 2.3%, respectively. Fu *et al.* [25] solution enhances the complexity

TABLE V
 Δ ET AND BD-BR PERFORMANCE OF THE PROPOSED SOLUTION IN COMPARISON WITH STATE-OF-THE-ART TECHNIQUES IN AI CODING CONFIGURATION.

Class	Sequence	Fu <i>et al.</i> [25], VTM1.0		Chen <i>et al.</i> [27], VTM4.0		Li <i>et al.</i> [17], VTM7.0		Ours top-3, VTM10.2		Ours top-2, VTM10.2	
		BD-BR	Δ ET	BD-BR	Δ ET	BD-BR	Δ ET	BD-BR	Δ ET	BD-BR	Δ ET
Class A1	Tango2	1.47%	54%	1.38%	48.7%	1.52%	40.8%	0.54%	46.7%	1.51%	66.4%
	FoodMarket4	1.01%	53%	0.84%	30.3%	1.26%	42.2%	0.53%	47.5%	1.45%	66.2%
	Campfire	1.06%	46%	1.29%	49.1%	2.02%	48.7%	0.74%	48.3%	2.01%	67%
	Average	1.18%	51%	1.17%	42.7%	1.6%	43.9%	0.6%	47.5%	1.66%	66.5%
Class A2	CatRobot1	1.58%	43%	1.99%	50.4%	2.16%	45.4%	0.99%	46.1%	2.6%	66.9%
	DaylightRoad2	1.49%	49%	2%	54.1%	1.16%	49.4%	1.02%	50.6%	2.55%	73.5%
	ParkRunning3	0.58%	51%	0.8%	40.6%	1.15%	41.7%	0.38%	42.6%	0.95%	59.5%
	Average	1.22%	47.7%	1.6%	48.4%	1.49%	45.5%	0.8%	46.4%	2.03%	66.6%
Class B	MarketPlace	0.60%	52%	-	-	0.8%	46.6%	0.53%	55.6%	1.36%	75.8%
	RitualDance	1.08%	45%	-	-	1.07%	44.9%	0.87%	51.7%	2.5%	73%
	Cactus	0.92%	44%	1.73%	49.8%	1.12%	49.3%	0.89%	49.4%	2.65%	72.4%
	BasketballDrive	0.89%	49%	1.54%	50.1%	1.64%	52%	0.92%	51.6%	2.57%	73%
	BQTerrace	0.78%	48%	1.4%	56%	1.11%	45.6%	1.06%	46.5%	2.82%	72%
	Average	0.85%	47.6%	1.56%	52%	1.15%	47.7%	0.85%	51%	2.38%	73.2%
Class C	RaceHorses	0.77%	42%	1.35%	50.6%	0.96%	46.5%	0.66%	46.2%	2.08%	74.5%
	BQMall	0.94%	39%	2.12%	58.9%	1.17%	49.8%	1.01%	47%	3.2%	75.8%
	PartyScene	0.53%	42%	1.01%	51%	0.61%	45.2%	0.58%	44.1%	2.21%	74.3%
	BasketballDrill	1.91%	46%	2.05%	54.8%	1.63%	39.3%	1.6%	45.4%	4.75%	73%
	Average	1.04%	42.3%	1.63%	53.8%	1.09%	45.2%	0.96%	45.7%	3.06%	74.4%
Class D	RaceHorses	0.91%	39%	1.28%	54.7%	1.2%	41.6%	0.67%	43.6%	2.46%	65.6%
	BQSquare	0.51%	44%	0.75%	52.8%	0.74%	44.5%	0.61%	44.4%	2.49%	69.7%
	BlowingBubbles	0.61%	37%	1.4%	54.9%	0.92%	41.6%	0.64%	40.5%	2.48%	64.9%
	BasketballPass	0.75%	43%	1.77%	53.1%	1.41%	44.5%	0.9%	44.5%	2.94%	65.9%
	Average	0.7%	40.8%	1.3%	53.9%	1.07%	43.1%	0.7%	43.3%	2.59%	66.5%
Class E	FourPeople	1.26%	41%	2.71%	56.3%	1.33%	49.9%	1.2%	44.7%	3.64%	71%
	Johnny	1.44%	39%	2.77%	55.8%	2.33%	48.2%	1.42%	42.6%	3.97%	67.4%
	KristenAndSara	1.27%	40%	2.17%	52.8%	1.76%	50.5%	1.06%	44.4%	3.47%	68.5%
	Average	1.32%	40%	2.55%	55%	1.81%	49.5%	1.23%	43.9%	3.69%	69%
Average		1.02%	44.8%	1.62%	51.2%	1.32%	45.8%	0.86%	46.6%	2.57%	69.8%
Class F	ArenaOfValor	-	-	-	-	-	-	1.08%	22%	3.38%	49.7%
	BasketballDrillText	-	-	2.09%	56.3%	-	-	1.59%	22.5%	4.69%	52.5%
	SlideEditing	-	-	0.52%	45.4%	-	-	1.21%	27.3%	4.67%	58.8%
	SlideShow	-	-	2.11%	45.8%	-	-	1.5%	26%	4.85%	56.2%
	Average	-	-	1.57%	49.2%	-	-	1.34%	24.5%	4.4%	54.3%

reduction by 2.4% at the expense of a high BD-BR increase of 0.5% compared to our top-3 configuration. Concerning the B class videos, our top-3 configuration is able to halve the complexity reduction with 51% of complexity reduction for less than one percent of BD-BR increase i.e. 0.85%. The closest to our method is Fu *et al.* [27] technique achieving similar BD-BR scores but at lower complexity reduction by 3.4%. Our top-2 configuration enables 73.2% complexity reduction for 2.38% BD-BR increase. The highest performance in terms of both complexity reduction and BD-BR increase are obtained for the *MarketPlace* sequence. Indeed, the proposed method in top-3 and top-2 configurations reaches 55.6% and 75.8% complexity reductions for 0.53% and 1.36% BD-BR increases, respectively.

For lower resolution classes C to E, the top-3 configuration achieves in average less than 1% BD-BR increase for a maximum of 47% complexity reduction. Compared to Fu *et al.* [25], our method has lower BD-BR increase for higher complexity reduction through all lower resolution classes. Li *et al.* [17] has higher BD-BR increase for lower complexity reduction for class C and D compared to our top-3 configuration. For class E, Li *et al.* [17] solution obtained 5.6% more complexity reduction but at the cost of 0.58% BD-BR increase compared to our method. Chen *et al.* [27] almost doubled the BD-BR loss with 1.76% for a complexity reduction increase of 9.9% compared to our top-3 configuration through low resolution

classes. In the case of the top-2 configuration, low resolutions have lower performance compared to high resolutions. In fact, this approach on low resolution contents including classes C, D and E reaches the complexity of high resolution contents (classes A1, A2 and B) of 70.1% for higher BD-BR loss of 3.06% which is higher by approximately 1% compared to the BD-BR loss of high resolutions contents (2.09%). Low resolution contents result in deeper partitions, so the more the complexity is reduced, the less space is available to skip splits. As the global partition is composed of more split, the impact on BD-BR is more significant at high complexity reductions.

The class F has specific sequences with screen content such as slides or gaming content. Our method is not optimized for this type of contents, since these contents have not been considered in the learning process. However, our approach still achieves 24.5% complexity reduction for 1.34% BD-BR increase. Chen *et al.* [27] are the only one to report results on class F with three out of four sequences. In average, they got higher complexity reduction but for a higher BD-BR increase. Adding screen content to the training dataset could be a solution to overcome state-of-the-art techniques.

Fig. 10 shows the performance of our method in complexity reduction versus BD-BR jointly with state-of-the-art techniques in a 2D plan on CTC classes except class F. In addition to the configurations presented in the table, two new specific configurations have been included. The selection of

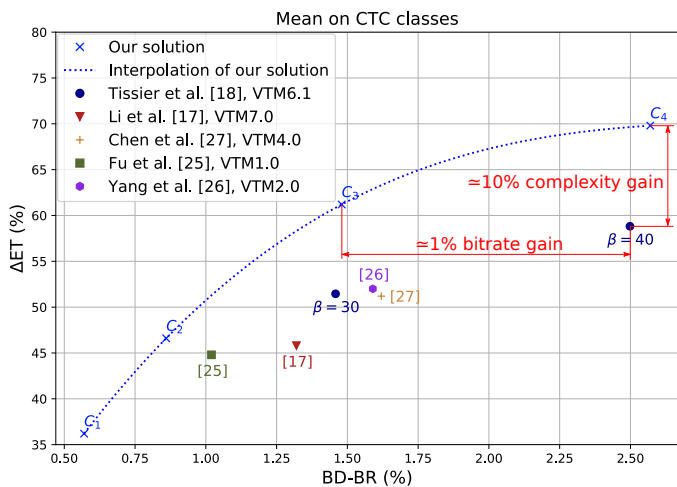


Fig. 10. Complexity reduction versus BD-BR performance comparison between the proposed method and state-of-the-art techniques on CTC classes except class F (AI configuration). An interpolation curve over our four configurations is plotted in blue dot line

top-3 for the multi-classification with 6 possibilities and top-4 for the other DT LGBM models is defined as C_1 . The top-3 configuration is defined as C_2 . The top-3 for all DT LGBM models except the multi-classification with 6 possibilities for which top-2 is used in configuration C_3 , and finally, top-2 for all DT models is defined as C_4 . These several configurations reach different trade-offs of complexity reduction for each specific BD-BR loss which allows us to draw and interpolation curve over these four configurations. This interpolation help us to compare the results since the rate-distortion-complexity trade-offs are not linear. It allows a comparison at each point of complexity reduction or BD-BR increase of our method. As explained through the previous table, the figure confirms that our solution outperforms the best performing state-of-the-art techniques. The points representing the other solutions are all below the interpolation curve of our approach. At the same BD-BR loss, we achieve a complexity reduction of 6.5%, 12.5%, 10.1% and 12.1% compared to Fu *et al.* [25], Li *et al.* [17], Yang *et al.* [26] and Chen *et al.* [27] techniques, respectively. For the same complexity reduction, we obtain a BD-BR gain of 0.21%, 0.49%, 0.54% and 0.61% against Fu *et al.* [25], Li *et al.* [17], Yang *et al.* [26] and Chen *et al.* [27] techniques, respectively.

The solution proposed in [18] is also illustrated in this figure to show the interest of our new proposal in terms of performance gain. Two configurations of the previous solution were selected with decision thresholds: $\beta = 30$ and $\beta = 40$. Our C_3 and C_4 configurations are better than the $\beta = 30$ and $\beta = 40$ solutions with a gain in complexity reduction of approximately 10% for a similar BD-BR loss. Compared to $\beta = 40$ which reaches 58.8% complexity reduction, our solution C_3 affords a significant BD-BR gain of 1.02%.

D. Complexity overhead

In this section, the complexity overhead of the CNN and DT inference is investigated under the VTM. Table VI presents the time spent in the CNN and in the DT predictions for

C_2 configuration in comparison with the VTM10.2 anchor encoding time. These values are obtained by applying a ratio between the CNN or DT time and the VTM reference encoding time. The execution time of the CNN inference is in average lower than the execution time of the DT model. Indeed, even if the CNN inference is higher, the DT infers at each CU size unlike the CNN which is carried-out only once for each 64×64 CU. The execution time ratio of the CNN is higher in the Ultra High Definition (UHD) classes especially the class A1. This can be a result of the early skip methods integrated in the VTM that leads to shallow partition, i.e. less time in the encoding process. Moreover, the results for the DT inference time is homogeneous through all the CTC classes. In average, both execution times of the CNN and DT are under 2% and taken together, they require less than 3% of the encoding time. These results show that the prediction times are negligible, especially since the CNN and DT models can be optimized, accelerated or parallelized. Especially, the execution time of the CNN can be significantly reduced by targeting a GPU or completely removed when parallelizing the CNN inference with the RDO.

VII. CONCLUSION

In this paper we have proposed a two stage CNN and DT method to reduce the complexity of the VTM encoder in AI configuration. The CNN is designed to predict a CU partition through a vector of probabilities based on the local property of the block. This vector considered as spatial features is then passed as input to the DT model that predicts the split probabilities at each CU depth. The DT method integrated after the CNN inference benefits from all the probabilities inside the CU instead of taking only the probabilities at the spatial location of the split. Depending on the selected configuration, a top-N probability selection is performed on the DT output to skip the unlikely splits.

Our proposed method outperforms state-of-the-art techniques in terms of trade-off between complexity reduction and coding loss. Concerning the top-3 configuration, our proposal assessed on the VVC CTC sequences enabled in average 46.6% complexity reduction for a negligible BD-BR loss of 0.86%. The top-2 configuration was able to reach a higher complexity reduction of 69.8% for 2.57% BD-BR loss. These promising results motivated us to extend our method to the RA configuration. This extension investigated as future work will require to take advantage of the motion flow among adjacent frames.

REFERENCES

- [1] Cisco, “Cisco Visual Networking Index : Forecast and Trends, 2017-2022,” Tech. Rep., 2019.
- [2] H. O. Domínguez and K. R. Rao, *Versatile Video Coding Latest Advances in Video Coding Standards*, pp. i–xxx, 2018.
- [3] D. García-Lucas, G. Cebrián-Márquez, and P. Cuenca, “Rate-distortion/complexity analysis of HEVC, VVC and AV1 video codecs,” *Multimedia Tools and Applications*, Aug. 2020.
- [4] Fan Zhang, Angeliki V. Katsenou, Mariana Afonso, Goce Dimitrov, and David R. Bull, “Comparing VVC, HEVC and AV1 using Objective and Subjective Assessments,” *arXiv:2003.10282 [eess]*, Mar. 2020, arXiv: 2003.10282.

TABLE VI
OVERHEADS OF THE CNN AND DT LGBM (IN %) FOR C_2 CONFIGURATION WITH RESPECT TO THE EXECUTION TIME OF THE VTM ANCHOR.

	Class A1	Class A2	Class B	Class C	Class D	Class E	Class F	Average
CNN overhead	2.7%	1.2%	1%	0.6%	0.5%	1.4%	1.2%	1.2%
DT overhead	2%	1.7%	1.7%	1.6%	1.6%	1.8%	1.6%	1.7%
Total	4.7%	2.9%	2.7%	2.2%	2.1%	3.2%	2.8%	2.9%

- [5] Frank Bossen, Xiang Li, and Karsten Suehring, "AHG report: Test model software development (AHG3)," *JVET-T0003*, Oct. 2020.
- [6] A. Wieckowski, J. Ma, H. Schwarz, D. Marpe, and T. Wiegand, "Fast Partitioning Decision Strategies for The Upcoming Versatile Video Coding (VVC) Standard," in *2019 IEEE International Conference on Image Processing (ICIP)*, Sept. 2019, pp. 4130–4134.
- [7] Edouard François, Michel Kerdranvat, Rémi Jullian, and Christophe Chevanec, "VVC PER-TOOL PERFORMANCE EVALUATION COMPARED TO HEVC," p. 14.
- [8] Mario Saldanha, Gustavo Sanchez, Cesar Marcon, and Luciano Agostini, "Complexity Analysis Of VVC Intra Coding," in *2020 IEEE International Conference on Image Processing (ICIP)*, Abu Dhabi, United Arab Emirates, Oct. 2020, pp. 3119–3123, IEEE.
- [9] A. Tissier, A. Mercat, T. Amestoy, W. Hamidouche, J. Vanne, and D. Menard, "Complexity Reduction Opportunities in the Future VVC Intra Encoder," in *2019 IEEE 21st International Workshop on Multimedia Signal Processing (MMSP)*, Kuala Lumpur, Malaysia, Sept. 2019, pp. 1–6, IEEE.
- [10] G. Correa, P. A. Assuncao, L. V. Agostini, and L. A. da Silva Cruz, "Fast HEVC Encoding Decisions Using Data Mining," *IEEE Transactions on Circuits and Systems for Video Technology*, vol. 25, no. 4, pp. 660–673, Apr. 2015.
- [11] Tianyi Li, Mai Xu, Xin Deng, and Liquan Shen, "Accelerate CTU Partition to Real Time for HEVC Encoding With Complexity Control," *IEEE Transactions on Image Processing*, vol. 29, pp. 7482–7496, 2020.
- [12] A. Mercat, F. Arrestier, M. Pelcat, W. Hamidouche, and D. Menard, "Machine Learning Based Choice of Characteristics for the One-Shot Determination of the HEVC Intra Coding Tree," in *2018 Picture Coding Symposium (PCS)*, June 2018, pp. 263–267.
- [13] Somdyuti Paul, Andrey Norkin, and Alan C. Bovik, "Speeding up VP9 Intra Encoder with Hierarchical Deep Learning Based Partition Prediction," *IEEE Transactions on Image Processing*, vol. 29, pp. 8134–8148, 2020, arXiv: 1906.06476.
- [14] Mai Xu, Tianyi Li, Zulin Wang, Xin Deng, Ren Yang, and Zhenyu Guan, "Reducing Complexity of HEVC: A Deep Learning Approach," *IEEE Transactions on Image Processing*, vol. 27, no. 10, pp. 5044–5059, Oct. 2018, arXiv: 1710.01218.
- [15] Z. Wang, S. Wang, J. Zhang, S. Wang, and S. Ma, "Probabilistic Decision Based Block Partitioning for Future Video Coding," *IEEE Transactions on Image Processing*, vol. 27, no. 3, pp. 1475–1486, Mar. 2018.
- [16] Thomas Amestoy, Alexandre Mercat, Wassim Hamidouche, Daniel Menard, and Cyril Bergeron, "Tunable VVC Frame Partitioning Based on Lightweight Machine Learning," *IEEE Transactions on Image Processing*, vol. 29, pp. 1313–1328, 2020.
- [17] Tianyi Li, Mai Xu, Runzhi Tang, Ying Chen, and Qunliang Xing, "DeepQMT: A Deep Learning Approach for Fast QMT-based CU Partition of Intra-mode VVC," *arXiv:2006.13125 [cs, eess]*, July 2020, arXiv: 2006.13125.
- [18] A. Tissier, W. Hamidouche, J. Vanne, F. Galpin, and D. Menard, "CNN Oriented Complexity Reduction of VVC Intra Encoder," in *2020 IEEE International Conference on Image Processing (ICIP)*, Abu Dhabi, United Arab Emirates, Oct. 2020, pp. 3139–3143, IEEE.
- [19] Meng Wang, Junru Li, Li Zhang, Kai Zhang, Hongbin Liu, Shiqi Wang, Sam Kwong, and Siwei Ma, "Extended Coding Unit Partitioning for Future Video Coding," *IEEE Transactions on Image Processing*, vol. 29, pp. 2931–2946, 2020.
- [20] Qiuwen Zhang, Yihan Wang, Lixun Huang, and Bin Jiang, "Fast CU Partition and Intra Mode Decision Method for H.266/VVC," *IEEE Access*, vol. 8, pp. 117539–117550, 2020.
- [21] Ting Fu, Hao Zhang, Fan Mu, and Huanbang Chen, "Two-Stage Fast Multiple Transform Selection Algorithm for VVC Intra Coding," in *2019 IEEE International Conference on Multimedia and Expo (ICME)*, Shanghai, China, July 2019, pp. 61–66, IEEE.
- [22] Biao Min and Ray C. C. Cheung, "A Fast CU Size Decision Algorithm for the HEVC Intra Encoder," *IEEE Transactions on Circuits and Systems for Video Technology*, vol. 25, no. 5, pp. 892–896, May 2015.
- [23] Z. Wang, S. Wang, J. Zhang, S. Wang, and S. Ma, "Effective Quadtree Plus Binary Tree Block Partition Decision for Future Video Coding," in *2017 Data Compression Conference (DCC)*, Apr. 2017, pp. 23–32.
- [24] Z. Jin, P. An, L. Shen, and C. Yang, "CNN oriented fast QTBT partition algorithm for JVET intra coding," in *2017 IEEE Visual Communications and Image Processing (VCIP)*, Dec. 2017, pp. 1–4.
- [25] Ting Fu, Hao Zhang, Fan Mu, and Huanbang Chen, "Fast CU Partitioning Algorithm for H.266/VVC Intra-Frame Coding," in *2019 IEEE International Conference on Multimedia and Expo (ICME)*, Shanghai, China, July 2019, pp. 55–60, IEEE.
- [26] H. Yang, L. Shen, X. Dong, Q. Ding, P. An, and G. Jiang, "Low Complexity CTU Partition Structure Decision and Fast Intra Mode Decision for Versatile Video Coding," *IEEE Transactions on Circuits and Systems for Video Technology*, pp. 1–1, 2019.
- [27] Fen Chen, Yan Ren, Zongju Peng, Gangyi Jiang, and Xin Cui, "A fast CU size decision algorithm for VVC intra prediction based on support vector machine," *Multimedia Tools and Applications*, July 2020.
- [28] Jinchao Zhao, Yihan Wang, and Qiuwen Zhang, "Adaptive CU Split Decision Based on Deep Learning and Multifeature Fusion for H.266/VVC," *Scientific Programming*, vol. 2020, pp. 1–11, Aug. 2020.
- [29] M. Lei, F. Luo, X. Zhang, S. Wang, and S. Ma, "Look-Ahead Prediction Based Coding Unit Size Pruning for VVC Intra Coding," in *2019 IEEE International Conference on Image Processing (ICIP)*, Sept. 2019, pp. 4120–4124.
- [30] Benjamin Bross, Paul Keydel, Heiko Schwarz, Detlev Marpe, Thomas Wiegand, Liang Zhao, Xin Zhao, Xiang Li, Shan Liu, Yao-jen Chang, Hui-yu Jiang, Po-han Lin, Chi-chang Kuo, Ching-chieh Lin, and Chun-lung Lin, "Multiple reference line intra prediction," *JVET-L0283*, Sept. 2018.
- [31] Kaiping He, Xiangyu Zhang, Shaoqing Ren, and Jian Sun, "Deep Residual Learning for Image Recognition," *arXiv:1512.03385 [cs]*, Dec. 2015, arXiv: 1512.03385.
- [32] Mingxing Tan and Quoc V. Le, "EfficientNet: Rethinking Model Scaling for Convolutional Neural Networks," *arXiv:1905.11946 [cs, stat]*, May 2019, arXiv: 1905.11946.
- [33] Karen Simonyan and Andrew Zisserman, "Very Deep Convolutional Networks for Large-Scale Image Recognition," *arXiv:1409.1556 [cs]*, Apr. 2015, arXiv: 1409.1556.
- [34] Guolin Ke, Qi Meng, Thomas Finley, Taifeng Wang, Wei Chen, Weidong Ma, Qiwei Ye, and Tie-Yan Liu, "LightGBM: A Highly Efficient Gradient Boosting Decision Tree," *Advances in Neural Information Processing Systems 30*, p. 9, 2017.
- [35] Eirikur Agustsson and Radu Timofte, "NTIRE 2017 Challenge on Single Image Super-Resolution: Dataset and Study," in *2017 IEEE Conference on Computer Vision and Pattern Recognition Workshops (CVPRW)*, Honolulu, HI, USA, July 2017, pp. 1122–1131, IEEE.
- [36] Evgeniu Makov, *Dataset image 4k*, 2019.
- [37] Iec Jtc and Itu-T Sg, "Call for evidence on learning-based image coding technologies (JPEG AI)," p. 15, 2020.
- [38] Samuel W. Hasinoff, Dillon Sharlet, Ryan Geiss, Andrew Adams, Jonathan T. Barron, Florian Kainz, Jiawen Chen, and Marc Levoy, "Burst photography for high dynamic range and low-light imaging on mobile cameras," *ACM Transactions on Graphics*, vol. 35, no. 6, pp. 1–12, Nov. 2016.
- [39] Radu Timofte and al., "NTIRE 2017 Challenge on Single Image Super-Resolution: Methods and Results," p. 12.
- [40] François Chollet et al, *Keras*, 2015.
- [41] Martin Abadi et al, "TensorFlow: Large-Scale Machine Learning on Heterogeneous Distributed Systems," p. 19.
- [42] Diederik P. Kingma and Jimmy Ba, "Adam: A Method for Stochastic Optimization," *arXiv:1412.6980 [cs]*, Jan. 2017, arXiv: 1412.6980.
- [43] F. Bossen, J. Boyce, K. Suehring, X. Li, and V. Seregin, "JVET common test conditions and software reference configurations for SDR video," *JVET-M1010*, Jan. 2019.
- [44] Gisle Bjontegaard, "Calculation of average PSNR differences between RD-curves," *VCEG-M33*, Apr. 2001.
- [45] Tobias Hermann, *Frugally Deep*, 2018.